

The Beam Filling Error in the Nimbus 5 Electronically Scanning Microwave Radiometer Observations of Global Atlantic Tropical Experiment Rainfall

DAVID A. SHORT

Goddard Laboratory for Atmospheres, Greenbelt, Maryland

GERALD R. NORTH

Texas A&M University, College Station

A comparison of rain rates retrieved from the Nimbus 5 electronically scanning microwave radiometer (ESMR 5) brightness temperatures and observed from shipboard radars during the Global Atlantic Tropical Experiment (GATE) phase I shows that the beam filling error is the major source of discrepancy between the two. When averaged over a large scene (the GATE radar array, 400 km in diameter), the beam filling error is quite stable, being 50% of the observed rain rate. This suggests the simple procedure of multiplying retrieved rain rates by 2 (correction factor). A statistical model of the beam filling error is developed by envisioning an idealized instrument field-of-view that encompasses an entire gamma distribution of rain rates. A modeled correction factor near 2 is found for rain rate and temperature characteristics consistent with GATE conditions. The statistical model also suggests that (1) the correction factor varies from 1.5 to 2.5 for suppressed to enhanced tropical convective regimes and (2) decreases to 1.5 as the freezing level and average depth of the rain column decreases to 2.5 km.

1. INTRODUCTION

Efforts to obtain quantitative estimates of rain rate from satellite passive microwave measurements are hampered by a fundamental remote sensing problem. The sensor response (microwave brightness temperature) is not linearly proportional to rain rate [Lovejoy and Austin, 1980], while the sensor field-of-view (FOV) is large enough to encompass substantial rain rate inhomogeneity. These factors are especially relevant for observations from the single-channel Nimbus 5 electrically scanning microwave radiometer (ESMR 5), tuned to 19.35 GHz with a spatial resolution of 25×25 km at nadir [Wilheit, 1972]. The combination of nonlinear sensor response with FOV inhomogeneities results in retrieved rain rates being lower than true rain rates [Chiu *et al.*, 1988].

The retrieval error due to FOV inhomogeneities has been referred to as the beam filling error [Bell, 1987] and the nonbeam filling error [Barrett and Martin, 1981] to convey the sense that a satellite FOV is rarely filled with a uniform rain rate. In this paper the term "beam filling error" is used. It is strongly dependent on the variance of rain rate within the FOV, increasing as the variance increases [Chiu *et al.*, 1988]. For a collection of ESMR 5 observations over a tropical mesoscale convective complex, the beam filling error can be considered as a random variable with nonzero mean. Additional rain rate retrieval errors arise from instrumental noise and deviations of surface, atmospheric, and cloud conditions from those assumed in the rain rate retrieval model. The error sources also include vertical variations in rain rate and finite cloud geometries generally not assumed in simple cloud/precipitation models. The goal of this paper is to reveal the importance of the beam filling error compared with other sources of error in rain rates

retrieved from Nimbus 5 ESMR observations over the Global Atmospheric Research Program Atlantic Tropical Experiment (GATE). A statistical model that provides a quantitative interpretation of the average beam filling error is also introduced, and its sensitivity to variations of rain rate properties likely to be encountered in other parts of the world is examined.

2. DATA DESCRIPTION

The ESMR 5 instrument flew in a polar orbit aboard the Nimbus 5 spacecraft at an altitude of approximately 1100 km with equator crossing times near local noon and midnight. The phased array antenna scanned across the flight track in 78 steps, or beam positions, with a resolution of 25×25 km at nadir, increasing to 45×160 km at a 50° scan angle, measuring the horizontally polarized radiation at 19.35 GHz. Simple cloud/precipitation models predict that rain rates greater than 15 mm/h can produce an increase in the microwave brightness temperature of about 100 K as compared with the relatively uniform cold background temperature of the low-emissivity ocean [Wilheit, 1986]. The radiometric noise level of ESMR 5 observations was less than 2 K, allowing rain patterns to be clearly visible over oceans in photofacsimile images [e.g., Barrett and Martin, 1981]. With twice daily global coverage for calendar years 1973-1976, these data have been the source of numerous efforts to estimate rain rates over the oceans [Allison *et al.*, 1974; Rao *et al.*, 1976; Adler and Rodgers, 1977]. The ESMR 5 data have been reprocessed to correct serious Earth location errors and to identify instrument malfunction problems [Lee and Byerly, 1981].

The GATE radar rainfall data are a gridded composite from C band digital radars aboard the *Oceanographer* and *Researcher* vessels [Hudlow, 1979]. Radar snapshots are available for phases I and II approximately every 15 min over a 400-km-diameter circle centered at 8.5°N , 23.5°W at 4×4 km resolution. These radar data allow a closer radar-

Copyright 1990 by the American Geophysical Union.

Paper number 89JD01651.
0148-0227/90/89JD-01651\$05.00

The Beam Filling Error in the Nimbus 5 Electronically Scanning Microwave Radiometer Observations of Global Atlantic Tropical Experiment Rainfall

DAVID A. SHORT

Goddard Laboratory for Atmospheres, Greenbelt, Maryland

GERALD R. NORTH

Texas A&M University, College Station

A comparison of rain rates retrieved from the Nimbus 5 electronically scanning microwave radiometer (ESMR 5) brightness temperatures and observed from shipboard radars during the Global Atlantic Tropical Experiment (GATE) phase I shows that the beam filling error is the major source of discrepancy between the two. When averaged over a large scene (the GATE radar array, 400 km in diameter), the beam filling error is quite stable, being 50% of the observed rain rate. This suggests the simple procedure of multiplying retrieved rain rates by 2 (correction factor). A statistical model of the beam filling error is developed by envisioning an idealized instrument field-of-view that encompasses an entire gamma distribution of rain rates. A modeled correction factor near 2 is found for rain rate and temperature characteristics consistent with GATE conditions. The statistical model also suggests that (1) the correction factor varies from 1.5 to 2.5 for suppressed to enhanced tropical convective regimes and (2) decreases to 1.5 as the freezing level and average depth of the rain column decreases to 2.5 km.

1. INTRODUCTION

Efforts to obtain quantitative estimates of rain rate from satellite passive microwave measurements are hampered by a fundamental remote sensing problem. The sensor response (microwave brightness temperature) is not linearly proportional to rain rate [Lovejoy and Austin, 1980], while the sensor field-of-view (FOV) is large enough to encompass substantial rain rate inhomogeneity. These factors are especially relevant for observations from the single-channel Nimbus 5 electrically scanning microwave radiometer (ESMR 5), tuned to 19.35 GHz with a spatial resolution of 25×25 km at nadir [Wilheit, 1972]. The combination of nonlinear sensor response with FOV inhomogeneities results in retrieved rain rates being lower than true rain rates [Chiu *et al.*, 1988].

The retrieval error due to FOV inhomogeneities has been referred to as the beam filling error [Bell, 1987] and the nonbeam filling error [Barrett and Martin, 1981] to convey the sense that a satellite FOV is rarely filled with a uniform rain rate. In this paper the term "beam filling error" is used. It is strongly dependent on the variance of rain rate within the FOV, increasing as the variance increases [Chiu *et al.*, 1988]. For a collection of ESMR 5 observations over a tropical mesoscale convective complex, the beam filling error can be considered as a random variable with nonzero mean. Additional rain rate retrieval errors arise from instrumental noise and deviations of surface, atmospheric, and cloud conditions from those assumed in the rain rate retrieval model. The error sources also include vertical variations in rain rate and finite cloud geometries generally not assumed in simple cloud/precipitation models. The goal of this paper is to reveal the importance of the beam filling error compared with other sources of error in rain rates

retrieved from Nimbus 5 ESMR observations over the Global Atmospheric Research Program Atlantic Tropical Experiment (GATE). A statistical model that provides a quantitative interpretation of the average beam filling error is also introduced, and its sensitivity to variations of rain rate properties likely to be encountered in other parts of the world is examined.

2. DATA DESCRIPTION

The ESMR 5 instrument flew in a polar orbit aboard the Nimbus 5 spacecraft at an altitude of approximately 1100 km with equator crossing times near local noon and midnight. The phased array antenna scanned across the flight track in 78 steps, or beam positions, with a resolution of 25×25 km at nadir, increasing to 45×160 km at a 50° scan angle, measuring the horizontally polarized radiation at 19.35 GHz. Simple cloud/precipitation models predict that rain rates greater than 15 mm/h can produce an increase in the microwave brightness temperature of about 100 K as compared with the relatively uniform cold background temperature of the low-emissivity ocean [Wilheit, 1986]. The radiometric noise level of ESMR 5 observations was less than 2 K, allowing rain patterns to be clearly visible over oceans in photofacsimile images [e.g., Barrett and Martin, 1981]. With twice daily global coverage for calendar years 1973-1976, these data have been the source of numerous efforts to estimate rain rates over the oceans [Allison *et al.*, 1974; Rao *et al.*, 1976; Adler and Rodgers, 1977]. The ESMR 5 data have been reprocessed to correct serious Earth location errors and to identify instrument malfunction problems [Lee and Byerly, 1981].

The GATE radar rainfall data are a gridded composite from C band digital radars aboard the *Oceanographer* and *Researcher* vessels [Hudlow, 1979]. Radar snapshots are available for phases I and II approximately every 15 min over a 400-km-diameter circle centered at 8.5°N , 23.5°W at 4×4 km resolution. These radar data allow a closer radar-

Copyright 1990 by the American Geophysical Union.

Paper number 89JD01651.
0148-0227/90/89JD-01651\$05.00

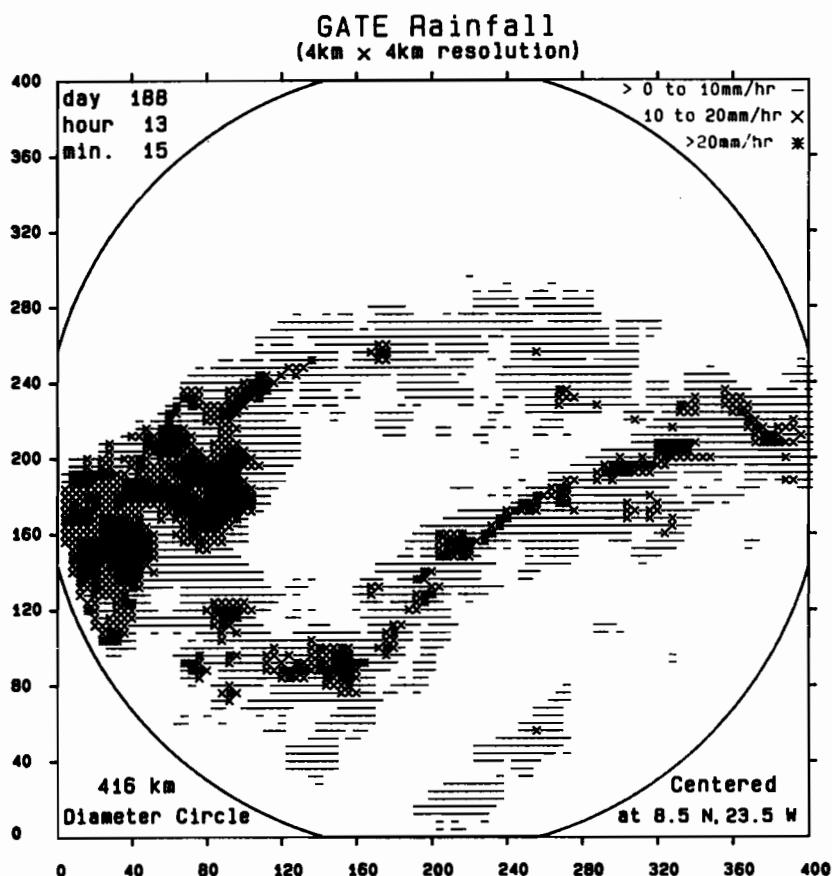


Fig. 1b. The radar rain rate pattern over the GATE area corresponding to the ESMR 5 overflight of Figure 1a. The 4×4 km resolution data are represented here in three categories (>0 – 10 , 10 – 20 , and >20 mm/h).

data that had been discarded (beyond the $\pm 30^\circ$ scan angle) in previous studies. The correction given by (1) is empirical. It may not apply in general to the ESMR 5 data set.

Two additional minor adjustments were made to the ESMR 5 brightness temperatures. Nighttime temperatures averaged 5 K colder than daytime, even under rain-free conditions. This range is too large to ascribe to diurnal variations in surface temperature or wind speed. Therefore, 5 K was added to the descending node temperatures. A careful inspection of Figures 1a and 1b reveals an offset of

the brightness temperature and rain rate patterns. The offset was apparently due to a flexure of the antenna mount caused by the spacecraft solar heating cycle. A location shift of less than 40 km was determined for each ESMR 5 overflight by an objective pattern correlation method [Short, 1988a]. The effects of each of the above corrections on FOV and scene-averaged rain rate retrievals is covered in detail by Short [1988a]. The location shift was most important for the FOV-scale comparisons. The correction dependent on scan angle markedly improved scene-averaged comparisons.

3. ESMR 5 RAIN RATE RETRIEVAL

For rain rate retrievals from ESMR 5 brightness temperatures the following functional approximation to the R , T curve from Wilheit [1986] for a freezing level of 4.5 km was used.

$$T = A - B \exp(-CR) - DR \quad (2)$$

where $A = 270$ K, $B = 100$ K, $C = 0.18$ h/mm, $D = 1.0$ h/mm, and R is in mm/h (see Figure 3). The exponential term represents increasing brightness temperature as rain rate and the optical depth of the rain layer increase. For a lower rain column height, T increases more slowly with R (C is smaller). The linear term approximates a decrease in brightness temperature due to scattering effects of a layer of cloud ice particles above the rain layer. The R , T data for (2) were taken from Wilheit [1986] with a modification for scattering from Kummerow [1987].

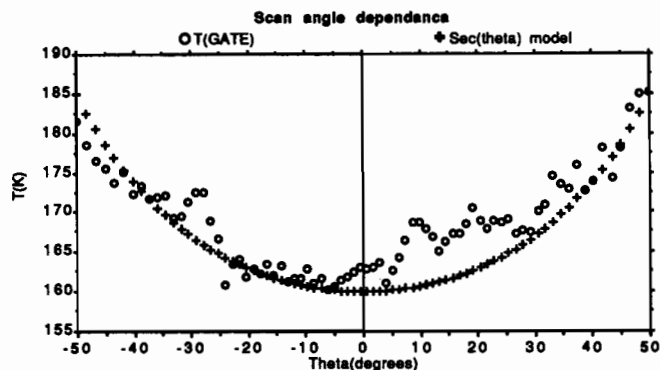


Fig. 2. Average brightness temperature versus scan angle for ESMR 5 observations over the GATE radar array during phase I. The smooth curve represents the secant (θ) form used to adjust all temperatures and reduce false rain retrievals.

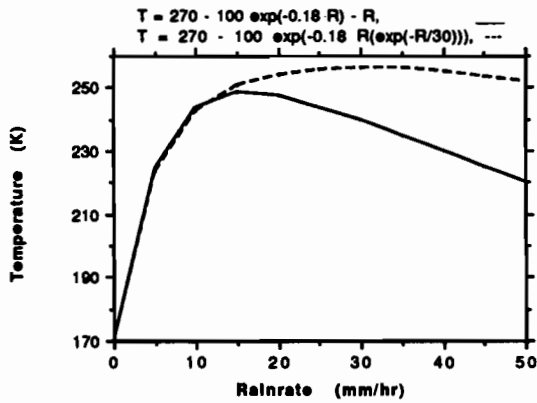


Fig. 3. The rain rate brightness temperature curve used to retrieve rain rates from ESMR 5 observations over the GATE area and to simulate brightness temperatures from the radar rain rate field (solid line). An R, T curve for effective rain layer thickness depending on rain rate (based on data from *Lovejoy and Austin* [1980], dashed line).

The cloud/precipitation model that (2) is based on does not include vertical gradients in rain rate. These cause the effective rain column height to vary [*Lovejoy and Austin*, 1980]. The dashed line in Figure 3 shows the T, R curve for $D = 0$ and C decreasing as rain rate increases according to $C(R) = 0.18 \exp(-R/30 \text{ h/mm})$ as suggested in data by *Lovejoy and Austin* [1980] for GATE. The two expressions agree closely over a range that covers more than 90% of the observed rain rates over GATE (0–15 mm/h). In section 4, indirect evidence of decreasing T at high rain rates is presented that supports (2) for the retrieval algorithm.

The validity of T, R curves from models that do not include the finite geometry of precipitating clouds may also be questioned. A verification of (2) as the average T, R relation was obtained by using (2) in a forward calculation, simulating T from the radar-rain rate field. This procedure is described in section 4.

For each ESMR 5 overflight of GATE a scene-averaged rain rate was inferred by numerically solving (2) for each ESMR 5 FOV temperature within the radar scene and averaging all the retrieved rain rates. The solution was always assumed to be on the low rain rate side of the double-valued function (2) because the single-channel ESMR 5 observations provided no information to indicate that the solution should be taken on the high rain rate side. In addition, the radar rain rate, averaged over an ESMR 5 FOV, rarely exceeded 15 mm/h. For $T < 170 \text{ K}$ the retrieved rain rate was 0.0 mm/h. Figure 4 shows the scene-averaged radar rain rates versus ESMR 5 rain rates for the 30 scenes. The satellite rain rates are consistently half as large as the radar rain rates and highly correlated, suggesting a correction factor of 2 for the retrieved rain rates. The standard error of estimate is 0.1 mm/h, giving a retrieval error of about 10% for the rainiest scenes and about 30% for the majority of low rain rate cases.

The high correlation shown in Figure 4 is encouraging. However, a note of caution is injected at this point. Empirically based retrievals from satellite visible and infrared observations also yield high correlations with ground truth rain rates when both are averaged over large areas [e.g., *Arkin*, 1979; *Woodley et al.*, 1980]. While the empirical retrievals have proven very useful, their coefficients provide

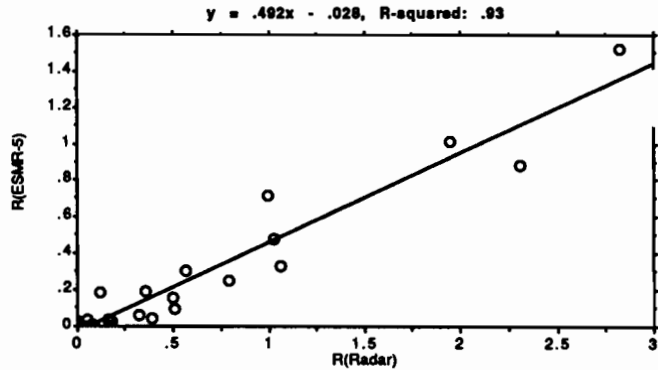


Fig. 4. Scene-averaged rain rates from radar versus ESMR 5 (in mm/h) for the 30 coincident scenes used in this study. ESMR 5 rain rates were retrieved for every observation that fell within the GATE 400-km radar circle.

little insight into the physical and statistical processes that make them work. This study concentrates on the slope in Figure 4 and the correction factor that it implies. In the following sections, physical and statistical arguments necessary for a quantitative understanding of the correction factor are developed. The dependence of the correction factor on the retrieval model (2) and rain rate distribution characteristics likely to be encountered in other areas is also explored.

4. BEAM FILLING ERROR VERSUS TOTAL ERROR

In order to compare the beam filling error to the total rain rate retrieval error, brightness temperatures for each rain FOV were simulated from the rain rate field. The simulated temperatures were then used to make a simulated rain rate retrieval (*Lovejoy and Austin* [1980] also simulated ESMR 5 retrieval errors but did not compare them to actual retrieval errors.) The simulated retrieval is less than the FOV-averaged radar rain rate due to inhomogeneities of rain rate within the FOV (the beam filling error). In contrast, rain rates retrieved from the ESMR 5 brightness temperatures differ from the radar rain rates due to a combination of all the error sources (beam filling, instrument noise, variable rain, cloud, and surface characteristics, collocation errors, radar errors). A direct comparison of the beam filling error and the total error can then be made. The simulation procedure is described first.

For each ESMR 5 brightness temperature greater than 170 K the radar pixel in the center of the FOV was located, and a weighted sum of temperatures from the surrounding pixels was calculated using

$$T(\text{simulated}) = \sum_{j=1}^N W_j [A - B \exp(-CR_j) - DR_j] \quad (3)$$

where the W_j are two-dimensional Gaussian weights and $A, B, C,$ and D are from (2). The weighting function has scan angle dependent half power points which match those given for the ESMR 5 antenna [*Wilheit*, 1972]. The summation was carried out to twice the distance of the half-power point including 95% of the weighting function volume. If the FOV was too close to the edge of the radar scene, T was not simulated. Figure 5 shows a scatterplot and linear regression of 511 simulated and observed temperatures. The high

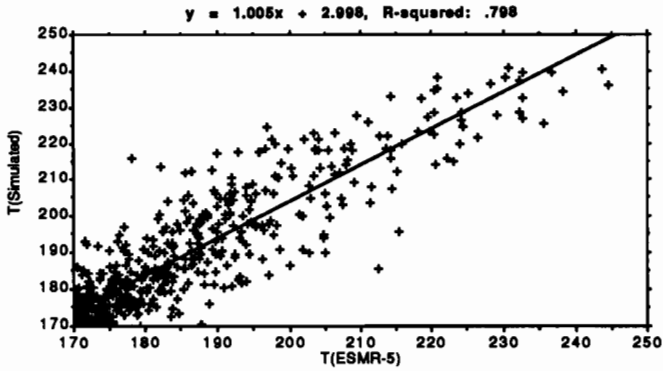


Fig. 5. Simulated versus observed brightness temperatures (in degrees K) for 511 rainy FOVs observed during GATE phase I.

correlation and slope indicate that (2) is a good approximation for the average cloud/precipitation conditions of GATE phase I. The standard error of simulated T , 8 K, is consistent with a 25% variation in C at a rain rate of 10 mm/h. This translates roughly into a 1-km variation in effective rain layer depth. A 1.5-km variation was found by *Lovejoy and Austin [1980]* in their analysis of radar volume scans.

Simulated temperatures average a few degrees warmer than observed, especially for the nadir view. This may be because rain-free radar pixels within the FOV were assumed to have a temperature of 170 K due to general cloudy conditions in the rainy areas. Apparently the nadir view offers a better opportunity to see the cool ocean surface between the rain/clouds. A slightly better fit could have been obtained by making the coefficients in (2) scan angle dependent. However, that level of complication would not add appreciably to the strength of the results presented here. Selection of the coefficients in (2) was guided mainly by physical reasoning. Some minor adjustments to D were made to bring the slope in Figure 5 close to 1. The improved agreement between simulated and observed temperatures as D was increased provides indirect evidence that scattering effects are important at the ESMR 5 frequency (19.35 GHz). An examination of the ESMR 5 data used in this study showed no local depressions in brightness temperature over areas of heavy rain. The ESMR 5 resolution appears to be too coarse to see such features.

Figure 6 shows the beam filling error versus the total rain rate retrieval error for each of the brightness temperature

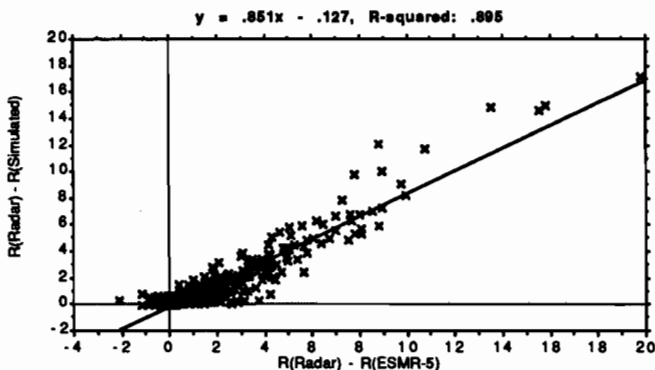


Fig. 6. Observed retrieval error versus the beam filling error (in mm/h) for the 511 rainy FOVs used in this study.

pairs in Figure 5. Note that retrieval errors for individual FOVs are highly variable and can be quite large (~ 20 mm/h). The small standard error of the beam filling error, 0.7 mm/h, indicates that FOV inhomogeneities of rain rate can explain a large range of the retrieval errors quite well. The simulated and observed errors are highly correlated, indicating that the beam filling error is the dominant part of the total error. The slope of the regression line is less than 1 due mainly to a cluster of points at low values below the regression line. These points are from the near nadir beam positions, where the simulated temperatures are generally higher than observed, giving a higher simulated retrieval and subsequently a lower error. The slope in Figure 6 is consistent with the observed 3 K average overestimation of T by the simulation algorithm. Again, the slope in Figure 6 could have been modified by making the coefficients of (2) scan angle dependent. However, the high correlation between simulated and observed errors is the point of significance, indicating that the beam filling error dominates over other sources of error in the rain rate retrieval.

5. STATISTICAL MODEL FOR THE BEAM FILLING ERROR

In the preceding section the beam filling error has been shown to dominate the errors in retrievals of rain rate from the ESMR 5 microwave brightness temperatures. The beam filling error can be corrected by multiplying retrieved rain rates by 2 (based on the slope and high correlation shown in Figure 5). A statistical model having a similar correction factor is developed below.

Consider an idealized instrument FOV that is completely filled with nonzero rain rates. A sampling of the FOV at infinitesimal resolution shows the rain rates to be exactly gamma distributed. This model concept has also been used in studies of statistical properties of microwave brightness temperatures [*Short, 1988b*] and area-averaged convective rainfall [*Atlas et al., this issue; Kedem et al., 1989*]. The gamma probability density function (pdf) is widely used to model rain rate statistics and has been tested as a descriptor of GATE radar rain rates [*Kedem et al., 1989*]. Analytic properties of the gamma pdf are especially useful in this development.

The brightness temperature for the ensemble FOV is found by integrating the transformation from R to T over the rain rate pdf:

$$E[T] = \int_0^{\infty} [A - B \exp(-Cr) - Dr] \cdot \left\{ \frac{1}{\Gamma(\alpha)\beta^\alpha} r^{\alpha-1} \exp(-r/\beta) \right\} dr$$

$$= A - B[(1 + \beta C)^{-\alpha}] - D\alpha\beta \quad (4)$$

where the term in braces is the gamma pdf, the lower term in square brackets is the gamma moment generating function, and $\alpha\beta$ is the average rain rate when raining. For the GATE phase I rain rates used here, $\alpha = 0.32$, $\beta = 12.43$ mm/h, $\alpha\beta = 3.98$ mm/h, $E[T] = 270$ K $- 68.66$ K $- 3.98$ K = 197.35 K, giving a retrieved rain rate of 1.94 mm/h and a correction factor (κ) of 2.05. This is in remarkable agreement with the empirical results of the previous section (Figure 4) and

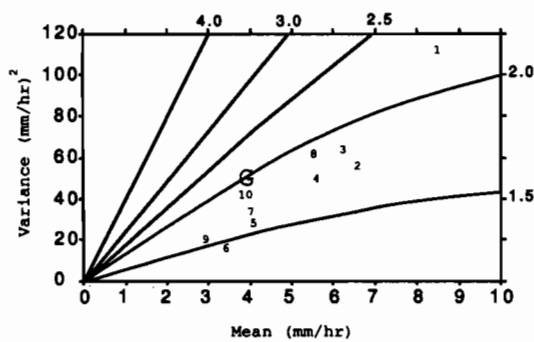


Fig. 7. Contours of the correction factor for the ensemble FOV model in coordinates of the mean rain rate where raining and the variance of rain rate where raining. The large G represents the ensemble rain rate distribution characteristics for GATE phase I. The small numbers represent the 10 rainiest scenes used in this study.

suggests that it may be possible to develop a generalized method for correcting ESMR 5 rain rates.

6. DISCUSSION

The ensemble FOV model can be used to provide some guidance on how κ may vary in other rain rate regimes. For this model, κ depends on the mean and variance of the gamma rain rate pdf. For a given mean and variance the gamma parameters are uniquely determined. Thus $E[T]$, given by (4), can be used to retrieve a rain rate and determine κ . Figure 7 shows contours of κ in the coordinates of mean and variance of rain rate. The large G indicates average conditions for GATE, phase I. The small numbers indicate conditions for the 10 rainiest scenes used in this study. The κ varies from 1.5 to 2.5 over the wide range of observed conditions. Notice that the contours of κ slope upward from low average rain rates with low variance to high average rain rates with high variance. This suggests that a nearly constant correction factor may apply over a wide range of rain rate regimes because high rain rates usually originate in convective clouds and are highly variable, while low rain rates usually occur in less variable stratiform clouds.

Figure 8 shows contours of κ for a rain column height near 2.5 km as would be found in higher latitudes ($A = 265$ K, $B = 115$ K, $C = 0.10$ h/mm, and $D = 1.0$ h/mm). The correction factors are smaller because the T , R relation is more linear at the heavily weighted low rain rates.

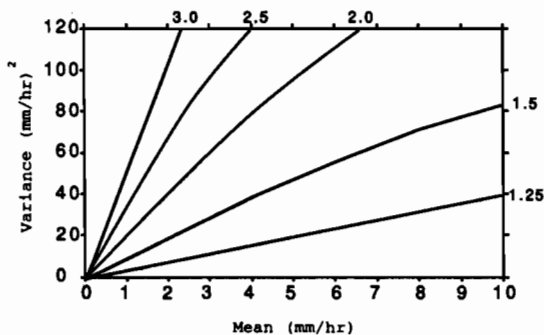


Fig. 8. Same as Figure 7 but for a retrieval model with $C = 0.10$ h/mm, simulating the correction factor (κ) for a 2.5-km rain column height.

The ensemble FOV model can also be used to estimate how errors in the retrieval model will impact the correction factor. Suppose the true value of D was 0.5 h/mm (50% less scattering effect than assumed). From (4) the "measured" temperature is 195.36 K, giving a retrieved rain rate of 1.75 mm/h (using the erroneous retrieval model) and a corrected rain rate of 3.57 mm/h (using the erroneous correction factor), a 10% underestimate. The small sensitivity to errors in D is encouraging because the amount of scattering due to cloud ice can be highly variable. On the other hand, a 25% error in C (approximately a 1-km error in the effective rain layer depth) results in a 25% error in the corrected rain rate. In the context of the retrieval technique used here, it is important to know the average value of C (or equivalently, the effective rain layer depth and its rain rate dependence) to the same accuracy required in the average retrieval. Variations in effective rain layer depth from its average value will cause large retrieval errors at the FOV scale; however, the average error due to this effect will be biased by only a few percent [Short, 1988a].

The ensemble FOV model can be modified to include a fraction (F) of the FOV having zero rain rate and/or to assume a lognormal distribution of rain rates [Short, 1988a]. The average ESMR 5 FOV is only about 60% covered by rain; however, the correction factor increases by only 10% when F is 0.6. Kedem *et al.* [1989] found that the lognormal pdf gave a better fit to GATE radar rain rates than the gamma pdf. A lognormal assumption decreases the correction factor by about 10% near G in Figure 7. Thus the ensemble FOV model suggests that the beam filling correction factor for GATE is 2.0 ± 0.5 over a wide range of conditions. The errors incurred by assuming a constant correction factor of 2.0 would be +33 to -20%.

It would be useful to repeat a study of this type for GATE phase III or any other oceanic radar/rain rate data set available for the ESMR 5 time frame (December 1972 to December 1976). A confirmation of physically plausible correction factors for ESMR 5 retrieved rain rates would motivate a global reanalysis of the ESMR 5 data set. Coincident T - R data sets from satellite and radar are more likely to be found during the Nimbus 7 scanning multichannel microwave radiometer (SMMR) lifetime (December 1978 to August 1987) or for the current Defense Meteorological Satellite Program's SSM/I; special sensor microwave imager (DMSP/SSM/I). The near 20 GHz channels on these instruments should provide ESMR 5 like observations that could be examined to determine beam filling errors and techniques to correct them.

This study has demonstrated that instantaneous area-averaged rain rate retrievals over GATE from the single-channel ESMR 5 can be corrected to an accuracy of about ± 0.1 mm/h, or $\pm 10\%$ for the rainiest scenes. This accuracy is obtainable with a single correction factor that accounts for the average beam filling error in the rain rate retrievals. While it may be possible to minimize the beam filling problem in multifrequency retrieval algorithms, these results should be encouraging to those who strive to improve rain rate retrievals from passive microwave observations past (ESMR 5, ESMR 6, the Nimbus 7 SMMR), present (the DMSP/SSM/I), and future (the proposed Tropical Rainfall Measuring Mission [Simpson *et al.*, 1988]).

Acknowledgment. It is a pleasure to thank B. Kedem for insights regarding statistical properties of area-averaged rain rate that he developed for presentation at the AGU 1986 Chapman Conference Rainfall Fields in Caracas, Venezuela.

REFERENCES

- Adler, R. F., and E. B. Rodgers, Satellite-observed latent heat release in a tropical cyclone, *Mon. Weather Rev.*, *105*, 956–963, 1977.
- Allison, L. J., E. B. Rodgers, T. T. Wilheit, and R. W. Fett, Tropical cyclone rainfall as measured by the Nimbus-5 electrically scanning radiometer, *Bull. Am. Meteorol. Soc.*, *55*, 1074–1089, 1974.
- Arkin, P. A., The relationship between fractional coverage of high cloud and rainfall accumulations during GATE over the B-scale array, *Mon. Weather Rev.*, *107*, 1382–1387, 1979.
- Atlas, D., D. Rosenfeld, and D. A. Short, The estimation of convective rainfall by area integrals, I, The theoretical and empirical basis, *J. Geophys. Res.*, this issue.
- Austin, P. M., and S. G. Geotis, Evaluation of the quality of precipitation data from a satellite-borne radiometer, final report under NASA grant NSG 5024, 30 pp., Mass. Inst. of Technol., Cambridge, 1978.
- Barrett, E. C., and D. W. Martin, *The Use of Satellite Data in Rainfall Monitoring*, 340 pp., Academic, San Diego, Calif., 1981.
- Bell, T. L., A space-time stochastic model of rainfall for satellite remote-sensing studies, *J. Geophys. Res.*, *92*, 9631–9643, 1987.
- Chiu, L. S., G. R. North, and D. A. Short, Errors in satellite rainfall estimation due to non-uniform field of view of space-borne microwave sensors, in *Proceedings of the IUGG Conference on Microwave Remote Sensing*, edited by A. Chedin, A. Deepak, Hampton, Va., 1988.
- Hudlow, M. D., Mean rainfall patterns for the three phases of GATE, *J. Appl. Meteorol.*, *18*, 1656–1669, 1979.
- Kedem, B., L. S. Chiu, and G. R. North, Estimation of mean rainrate: Application to satellite observations, *J. Geophys. Res.*, in press, 1989.
- Kummerow, C. D., Microwave radiances from horizontally finite, vertically structured precipitating clouds, Ph.D. thesis, Univ. of Wisc., Madison, 1987.
- Lee, D. K., and W. P. Byerly, Improvements to the Nimbus-5 ESMR calibrated brightness temperature data set, final report on NASA contract NAS5-25346, Syst. and Appl. Sci. Corp., Riverdale, Md., 1981.
- Lovejoy, S., and G. L. Austin, The estimation of rain from satellite-borne microwave radiometers, *Q. J. R. Meteorol. Soc.*, *106*, 255–276, 1980.
- Rao, M. S. V., W. V. Abbott, and J. S. Theon, Satellite-derived global oceanic rainfall atlas, *NASA Spec. Publ.*, *SP-410*, 1976.
- Short, D. A., Remote sensing of oceanic rain rates by passive microwave sensors: A statistical-physical approach, Ph.D. thesis, Texas A&M Univ., College Station, 1988a.
- Short, D. A., A statistical-physical interpretation of ESMR-5 brightness temperatures over the GATE area, in *Tropical Rainfall Measurements*, edited by J. S. Theon and N. Fugono, A. Deepak, Hampton, Va., 1988b.
- Simpson, J., G. R. North, and R. F. Adler, A proposed Tropical Rainfall Measuring Mission (TRMM) satellite, *Bull. Am. Meteorol. Soc.*, *69*, 278–295, 1988.
- Wilheit, T. T., The electrically scanning microwave radiometer (ESMR) experiment, in *The Nimbus-5 User's Guide*, edited by R. R. Sabatini, pp. 59–104, plus corrections, NASA Goddard Space Flight Center, Greenbelt, Md., 1972.
- Wilheit, T. T., Some comments on passive microwave measurement of rain, *Bull. Am. Meteorol. Soc.*, *67*, 1226–1232, 1986.
- Woodley, W. L., C. G. Griffith, and S. C. Stromatt, The inference of GATE convective rainfall from SMS-1 imagery, *J. Appl. Meteorol.*, *19*, 388–408, 1980.

G. R. North, Texas A&M University, College Station, TX 77843.
D. A. Short, Laboratory for Atmospheres, NASA Goddard Space Flight Center, Code 613, Greenbelt, MD 20771.

(Received November 14, 1988;
revised April 26, 1989;
accepted May 10, 1989.)